



Performance evaluation of downhole oil–water separators in wells that use DWL technique using computational fluid dynamics: influence of velocities and flow rates

Ahmad Buhamad¹ · Amir Hossein Saeedi Dehaghani¹

Received: 20 February 2023 / Accepted: 6 July 2023 / Published online: 21 July 2023
© The Author(s) 2023

Abstract

A major issue in many oil fields is the production of undesirable water from oil wells. One of the most important causes of unwanted water is water coning. This phenomenon may be leading to a decreasing oil production rate, an increasing water cut, and consequently high production costs. Downhole water loop (DWL) is a relatively new and effective technique to control water coning. Even though many studies have shown how effective the DWL approach is in reducing the problem of water cones, the issue of oil droplets escaping the drainage zone might damage the injection area and perhaps cause blockage. It is suggested to use the downhole oil–water separator (DOWS) approach to separate oil droplets from the water stream based on the difference in densities. This article gives a numerical analysis of DOWS in two stages. In order to confirm that the simulator could faithfully simulate this sort of separator, the findings of the employed simulator were first compared with the preceding analytical solutions. Then the impact of inlet velocities and flow rates was discussed numerically for seven scenarios in the second stage. The results showed that a high inlet velocity encourages the formation of oil droplets as a result of the mixture stream colliding with the separator walls, whereas a low inlet velocity produced undesirable results because the oil droplets remained dispersed in the water stream (the separation efficiency was 30.6% less than the high-velocity condition). In the following case, a novel design based on expanding the mixture input area and changing the mixture inlet and outlet points was presented to lessen the impact of mixture inlet velocity. The separation efficiency was improved by 38.65% as a result of this approach. Finally, the discussion's findings about the effect of mixture flow rates at the separator's inlet and upper outlet showed that the inlet rate has a bigger impact on separator performance than the upper outlet rate. The outcomes of this research and the numerical models can be utilized to enhance the system-level design, better understand this kind of separator, and increase its efficacy.

Keywords Numerical study · Down-hole oil · Water separators · Computational fluid dynamics · Oil–water separation · Two-phase flow

List of symbols

A	Cross-section area of the pipe (m^2)	D_{di}	Distance from water drainage perforation to water injection perforation (ft)
B_o	Oil volume factor (Rb/STB)	d_o	Oil droplet diameter (m)
B_w	Water volume factor (Rb/STB)	F_G	Gravity force (N)
c_o	Drift-flux profile parameter (dimensionless)	F_B	Buoyancy force (N)
DWS	Downhole water sink	F_D	Drag force (N)
DWL	Downhole water loop	f_o	Oil volume fraction (fraction)
DOWS	Down-hole oil/water separator	G	Gravitational constant ($9.8 m/s^2$)
		h_o	Oil zone thickness (ft)
		h_w	Water zone thickness (ft)
		K	Kinetic energy (m^2/s^2)
		k_o	Oil effective permeability (md)
		k_w	Water effective permeability (md)
		M	Mobility ratio
		n	Drift-flux exponent, dimensionless

✉ Amir Hossein Saeedi Dehaghani
asaeedi@modares.ac.ir

¹ Department of Petroleum Engineering, Faculty of Chemical Engineering, Tarbiat Modares University, Tehran 14115-143, Iran

P_k	Turbulent production ($\text{kg/m}^3 \text{s}$)
Q_{opc}	Critical oil production rate (Stb/d)
Q_{wdc}	Water drainage/injection rate (Stb/d)
Q_{wd}	Critical water drainage/injection rate (Stb/d)
Q_{op}	Oil production rate (Stb/d)
q_o	Oil rate (m^3/s)
Re_d	Oil droplet Reynolds number, dimensionless
r_e	Drainage radius (ft)
r_w	Well bore radius (ft)
U	Velocity component (m/s)
V_d	Drift velocity (when, $v_w = 0$, m/s)
V_o	In situ oil droplet velocity (m/s)
V_{wr}	Relative movement between the oil droplet and water column (m/s)
v_m	Average superficial mixture velocity (m/s)
v_w	In situ water velocity (m/s)
v_o	In situ oil droplet velocity (m/s)
v_{wc}	Critical in situ water velocity (m/s)
Z_{op}	Distance from top perforation to stable OWC (ft)
Z_{wd}	Distance from water drainage perforation to stable OWC (ft)
μ_D	Dimensionless viscosity group, dimensionless
μ_o	Oil viscosity (cp)
μ_w	Water viscosity (cp)
μ_i	Turbulent viscosity (Pa s)
μ_m	Mixture viscosity (cp)
σ_{ow}	Oil–water interfacial tension (dyne/cm)
ρ_w	Water density (kg/m^3)
ρ_o	Oil density (kg/m^3)
ρ_m	Mixture density (kg/m^3)
ε	Turbulent dissipation rate (m^2/s^3)
γ_w	Water relative density
γ_o	Oil relative density

Subscripts

di	Water drainage and re-injection completions
i	Generic spatial coordinate
j	Generic spatial coordinate
op	Oil production completion
opc	Critical oil production
o	Oil
ow	Oil and water
pw	Bottom perforation
po	Top perforation
wd	Water drainage completion
wdc	Critical water production
w	Water

Introduction

In a partially penetrated oil/gas well, the oil/water contact locally rises toward the perforated interval by a process known as water coning. This phenomenon happens when

the vertical component of the viscous force is greater than the net gravitational force (Abass and Bass 1988). Since 1935, a number of scholarly studies have addressed the subject of water cones and provided analytical mathematical models to pinpoint the critical flow that prevents the formation of the water cone (Høyland et al. 1989; Farmen et al. 1999; Safari et al. 2018; Guo et al. 1992; Tabatabaei et al. 2012). Numerous creative solutions have been developed to deal with the problem of water cones, such as downhole water sink (DWS) technology, which relies on producing water separately from oil to prevent water from flooding the oil area (Wojtanowicz et al. 1991; Arslan et al. 2003, 2004; Ould-amer et al. 2004; Arslan 2005; Johns et al. 2005; Zeidani et al. 2008; Utama 2008). Moreover, downhole water loop (DWL) technology relies on re-injecting the water produced from the drainage region to prevent low pressure in the reservoir (Wojtanowicz and Xu 1992; Jin and Wojtanowicz 2010b, 2011; Jin et al. 2010). Despite the DWL technique's positive outcomes, the issue of oil droplets escaping with water can damage the injection region (Jin and Wojtanowicz 2013, 2014; Bedrikovetsky et al. 2005). This problem, which is brought on by the reverse cone phenomenon, was addressed by Jin et al. (2010), who provided an analytical approach to identify the critical flow values that prevent the formation of a reverse cone. However, because of the varied geological context and the inaccuracy of the used data, analytical solutions might not be accurate. To separate the oil droplets that might emerge with the water circulation, Jin and Wojtanowicz (2013) suggested employing a well separator, which depends on the density difference to separate the oil from the water. No numerical analysis of this type of separator was available, and in particular, the impact of mixture inlet velocity and flow rates on separation efficiency was not examined, despite the vast number of publications that examined separators in the oil industry, such as Ghaffarkhah et al. (2019); Al-Kayiem et al. (2019); Refsnes et al. (2019). In this work, the influence of the inlet velocities and flow rates of well separators utilized with DWL is studied numerically, and a design to lessen the impact of the inlet velocity of the mixture on separator performance is suggested.

Mechanisms of DWL and DOWS

To prevent cone growth, Widmyer developed the downhole water sink (DWS) technique in 1955 (Widmyer 1958). In this technique, oil and water are produced separately through two production tubes. According to his suggestion, the top (the oil zone) and bottom (the water zone) perforations must be separated (Swisher and Wojtanowicz 1996; Bowlin et al. 1997; Shirman 1998). For lowering the amount of water produced in oil wells as a result of

applying the DWS technique, Wojtanowicz and Xu (1992) suggested the downhole water loop (DWL) technology. In this technology, in addition to the traditional completion in the oil zone, the water loop equipment is added in the water zone below the oil–water contact (OWC) as shown in Fig. 1C. This technology had the advantage of becoming a solution to the environmental compliance problem associated with the disposal of produced water (Jin and Wojtanowicz 2010a; Jin 2009). In other words, formation water might be kept away from oil-producing perforations, allowing for increased oil recovery per well with reservoir pressure maintenance.

The main problem is the occurrence of the reverse cone phenomenon (Fig. 1A), which occurs in the opposite direction of the water cone (Fig. 1B). This phenomenon occurs when the viscous force for the drainage completion (water) exceeds the viscous force for the top (oil) completion.

To ascertain the critical flow values at which no cone and no reverse cone formation occur, analytical models were proposed by Jin et al. (2010); in other words, only oil is produced by the higher perforation and only water is produced by the lower perforation, as follows:

$$Q_{opc} = \frac{Q_{wd}B_w h_o}{MB_o h_w} (1 - D_{di}) + \frac{0.003066 K_o h_o (\gamma_w - \gamma_o)}{\mu_o B_o \ln(r_e/r_w)} [Z_{op} - Z_{wd} + Z_{wd}D_{di}] \tag{1}$$

$$Q_{wdc} = \frac{Q_{op}MB_o h_w}{B_w h_o} \frac{1}{(1 - D_{di})} + \frac{0.003066 K_w h_w (\gamma_w - \gamma_o)}{\mu_w B_w \ln(r_e/r_w)} \frac{[Z_{wd} - Z_{op} + Z_{wd}D_{di}]}{(1 - D_{di})} \tag{2}$$

where Q_{opc} is the critical oil production rate (Stb/d), Q_{wd} is the water drainage/injection rate (Stb/d), Q_{wdc} is the critical water drainage/injection rate (Stb/d), and Q_{op} is the oil production rate (Stb/d).

The analytical models, however, become unreliable under conditions of heterogeneous geological environments or the unreliability of the geological data used in the studies, making it possible for oil droplets to escape with the water produced by the bottom perforation due to the reverse cone phenomenon. To solve this problem, Jin and Wojtanowicz (2013) suggested applying the DOWS approach, which uses the density difference concept to separate oil droplets from a water stream. A simplified schematic of the separator concept used with the DWL technique can be seen in Fig. 2B, where water and oil droplets enter from the inlet and separate inside the separator before the oil comes out from the top and the water from the bottom and are injected into the injection area using a pump (P).

The oil droplet is susceptible to three forces: gravity (F_G), buoyancy (F_B) and drag (F_D), as shown in Fig. 2A. Analytical solutions for the critical water flow values that enable the oil droplet to rise and exit toward the surface can be determined by evaluating these forces. Mathematical solutions, including the Drift-Flux model in Eqs. (3–7), were presented by Jin and Wojtanowicz (2013), where he conducted a laboratory experiment on a separator with a diameter of 57 mm and a distance between the oil and water inlets of 229 mm to determine the values of some constants such as c_o .

$$V_d = 1.53 \frac{(1 - f_o)^n}{\mu_D^{0.977}} \left[\frac{\sigma_{ow} g (\rho_w - \rho_o)}{\rho_w^2} \right]^{0.25} \tag{3}$$

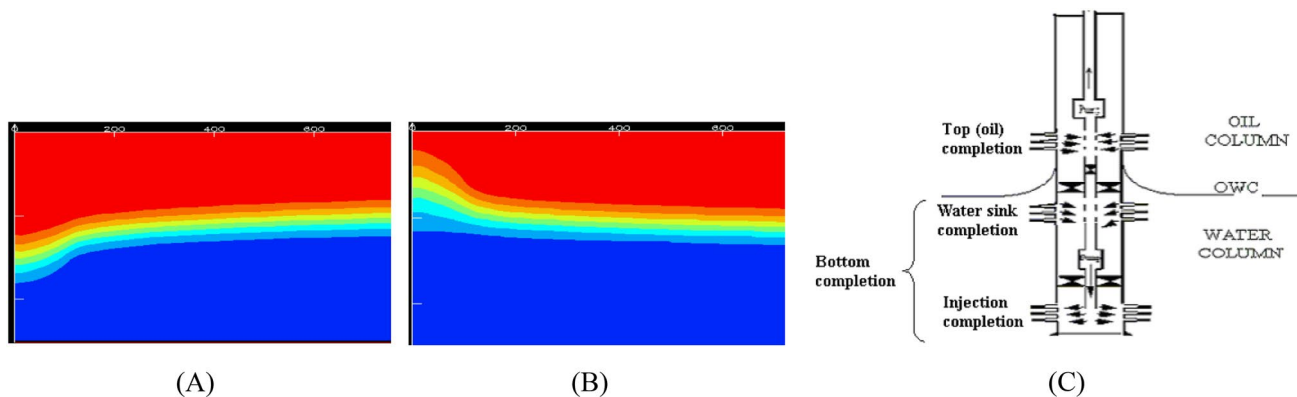
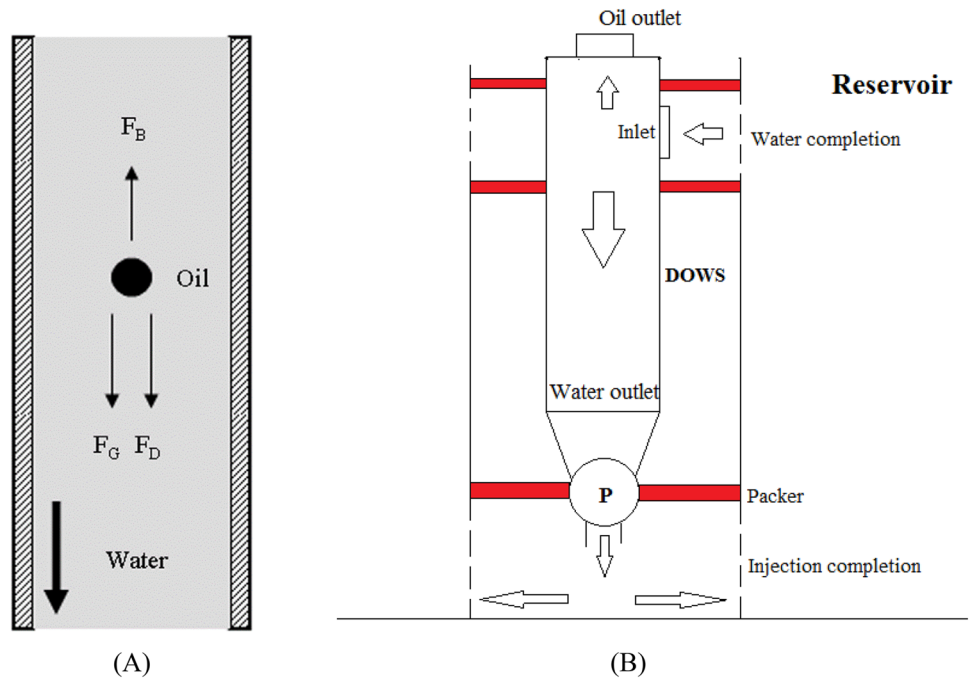


Fig. 1 A Oil saturation profile of the reverse cone (Inikori and Wojtanowicz 2001); B Oil saturation profile of the cone; C Schematic of the DWL completion (Jin 2009)

Fig. 2 **A** Forces acting on an oil droplet moving through a water stream (Jin and Wojtanowicz 2013); **B** DOWS schematic



$$f_o = \frac{q_o}{A \left[1.2v_m + 1.53 \left[\frac{\sigma_{ow}g(\rho_w - \rho_o)}{\rho_w^2} \right]^{0.25} \right]} \quad (4)$$

$$V_o = 1.53 \frac{(1-f_o)^n}{\mu_D^{0.977}} \left[\frac{\sigma_{ow}g(\rho_w - \rho_o)}{\rho_w^2} \right]^{0.25} - c_o v_w \quad (5)$$

$$V_{wc} = 1.53 \frac{(1-f_o)^n}{c_o \mu_D^{0.977}} \left[\frac{\sigma_{ow}g(\rho_w - \rho_o)}{\rho_w^2} \right]^{0.25} \quad (6)$$

$$\mu_D = \frac{2(2\mu_w + 3\mu_o)}{\mu_w + \mu_o} \quad (7)$$

where V_d is the drift velocity (when, $v_w = 0$, m/s), f_o is the oil volume fraction, V_o is the fraction in situ oil droplet velocity (m/s), V_{wc} is the critical in situ water velocity (m/s), μ_D is the dimensionless viscosity group, dimensionless, n is the drift-flux exponent, dimensionless ($n = 1$), c_o is the drift-flux profile parameter, dimensionless ($c_o = 1.235$).

Although the movement of the oil droplets within the water stream inside the separator is accurately described by these equations, they do not account for the inlet velocity, where the inlet velocity into the separator differs in value and direction from the velocity of the mixture inside the separator. As a result, we will use numerical solutions in this work to illustrate the impact of the inlet velocity into the separator and the flow rates.

Numerical study

Numerical simulations were performed using commercial CFD software, which provides the widest range of turbulence and physical models to accurately simulate. This work was done in two stages, the first of which was to demonstrate the commercial simulator's suitability for simulating this kind of separator. In the second stage, the impact of mixture inlet velocities and flow rates on separation efficiency will be discussed, and a design that addresses this issue will be presented. It is known that the flow pattern (laminar and turbulent) is determined by the Reynolds number Re_D (Jin and Wojtanowicz 2013):

$$Re_D = \frac{\rho_w |V_{wr}| d_o}{\mu_w} \quad (8)$$

$$|V_{wr}| = ||V_o| - |V_w|| \quad (9)$$

where ρ_w is the water density (kg/m³), V_o is the in situ oil droplet velocity (m/s), V_w is the in situ water velocity (m/s), μ_w is the water viscosity (pa·s), d_o is the oil droplet diameter (m).

The flow is laminar when the Reynolds numbers are less than 2000 and turbulent when they are greater than 4000 (Nayyar 2000). In this paper, turbulence was modeled using the Reynolds-averaged Navier-Stokes K-epsilon model, which has been applied to various investigations of gravity separators. The results it provided were quite close to actual field observations (Ghaffarkhah et al. 2018; Refsnes et al. 2019). Two extra conservation equations are

included in K-epsilon model, one for the turbulent kinetic energy k and the other for the turbulent dissipation rate ϵ :

$$\frac{\partial(\rho_m \cdot k)}{\partial t} + \frac{\partial}{\partial x_i}(U_i \cdot \rho_m \cdot k) = \frac{\partial}{\partial x_j} \left[\left(\frac{\mu_i}{\sigma_k} + \mu_m \right) \frac{\partial k}{\partial x_j} \right] - \rho_m \cdot \epsilon + P_k \tag{10}$$

$$\begin{aligned} \frac{\partial(\rho_m \cdot \epsilon)}{\partial t} + \frac{\partial}{\partial x_i}(U_i \cdot \rho_m \cdot \epsilon) &= \frac{\partial}{\partial x_j} \left[\left(\frac{\mu_i}{\sigma_\epsilon} + \mu_m \right) \frac{\partial \epsilon}{\partial x_j} \right] \\ &+ \frac{\epsilon}{k} \cdot (C_{\epsilon 1} \cdot P_k - C_{\epsilon 2} \cdot P_k \cdot \rho_m \cdot \epsilon) \end{aligned} \tag{11}$$

In these equations are, $C_{\epsilon 1}=1.44$, $C_{\epsilon 2}=1.92$, $\sigma_\epsilon=1.3$, and $\sigma_k=1$.

$$\mu_i = C_\mu \cdot \rho_m \cdot \frac{k^2}{\epsilon} \tag{12}$$

where $C_\mu=0.09$. P_k is the turbulence production due to viscous forces.

$$P_k = \mu_i \cdot \left(\frac{\partial U_i}{\partial x_j} + \frac{\partial U_j}{\partial x_i} \right) \cdot \frac{\partial U_j}{\partial x_i} \tag{13}$$

Stage 1: numerical model validation

The capability of the commercial CFD simulator utilized in this work will be confirmed by following a procedure similar to the laboratory experiment that was used to develop the analytical model Eqs. (3–7) and then contrasting the numerical findings with the analytical. To simulate the behavior of oil droplets in a water stream inside the separator, a geometric model for the studied separator, as shown in Fig. 3A, was built wherein

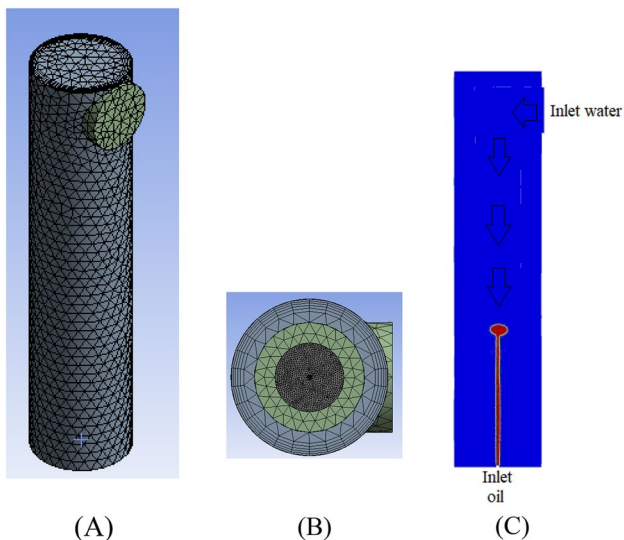


Fig. 3 A 3D shape of DOWS meshes; B Bottom view of meshes; and C A simplified diagram of the procedure applied in stage 1 (model validation)

the bottom inlet is used for oil and the upper inlet is used for water Fig. 3C. The oil inlet area is 3.14 mm², the water inlet area is 1256 mm², the bottom outlet area around the oil inlet is 1252.86 mm², the separator’s diameter is 57 mm, and the distance between the two inlets (oil and water) is 229 mm. Tetrahedron-type meshes, with a total of 1,061,733 cells, are widely dispersed in the oil inlet, as depicted in Fig. 3A, B. We used a variety of water flow values in the separator, as given in Table 1, for three different types of oil, whose attributes are shown in Table 2 (Jin and Wojtanowicz 2013). Then, we calculated the oil velocity values (V_o) for each water flow value by measuring the time at which the oil crossed between two fixed sites (the first is located at an altitude of 20 mm, and the second is at an altitude of 30 mm).

The outcomes are displayed in Fig. 4, where we observe the convergence with the analytical model’s outcomes (Eq. 5). Table 3 displays the boundary condition that was employed. Because the VOF model is appropriate for immiscible liquids like oil and water, it was utilized during this work to represent the oil–water multiphase flow in the separator. The primary (continuous) phase was water, while the secondary (dispersed) phase was oil. The viscosity model was also laminar at this stage. The coupled algorithm was used to achieve pressure–velocity coupling between continuity and momentum. Based on the least squared cell-based approach, gradients were discretized. PRESTO scheme was selected. QUICK was used to discretize momentum.

Table 1 The water velocity values and oil flow rates applied in stage 1 (model validation)

Water velocity, m/sec	Oil rate, 10 ⁻⁶ m ³ /min		
	Light mineral oil	Heavy mineral oil	#11 Oil
0.0	120	135	115
0.02	120	135	115
0.04	120	135	115
0.06	120	135	115
0.08	120	135	115
0.0949	–	–	115
0.1	120	135	–
0.12	120	–	–

Table 2 Specifications of primary (water) and secondary (oils) phases

Name	Density, ρ_o (kg/m ³)	Dynamic viscosity, μ_o (cp)	Oil/water interfacial tension, σ_{ow} (dyne/cm)
Light mineral oil	836.5	53.3	53
Heavy mineral oil	876.3	155	65
#11 Oil	905.7	373.4	36.9
Water used	1000	1	–

As we previously stated, the analytical model does not account for mixture inlet velocities, which, in our opinion, significantly affect the separator's performance. In order to understand how the mixture inlet velocities affected the process, we looked at stage 2.

Stage 2: effect of mixture inlet velocities and flow rates

At this stage, we will demonstrate the impact of the separator's inlet velocities and flow rates by running a simulation that is more similar to what occurs in the reverse cone where water and oil enter from the side inlet, causing separation to take place inside the separator, resulting in oil coming out of the upper outlet and water coming out of the lower outlet. We utilized the same software settings used in the first stage in all the cases investigated at this stage, with some alterations, whereas, in the first stage, the laminar model produced results close to the analytical calculations due to the low Reynolds number value, by substituting in Eq. 8, where the diameter of the oil droplet does not exceed 10 mm and the largest relative velocity does not exceed 0.15 m/s, i.e., the Reynolds number is roughly 1500. At this stage, the oil droplets are significantly larger, as we will see, and the mixture is moving at a high velocity of up to 0.4 m/s at the entrance area. Therefore, we used the turbulent model (K-epsilon model) at this stage. A contact angle ($\theta=170$ degree) is taken to account for the wetting behavior of the wall with the fluids. The time step size used is 0.004 s. We conducted all of our investigations at a processing time of

Table 3 Boundary conditions used in stage 1 (model validation)

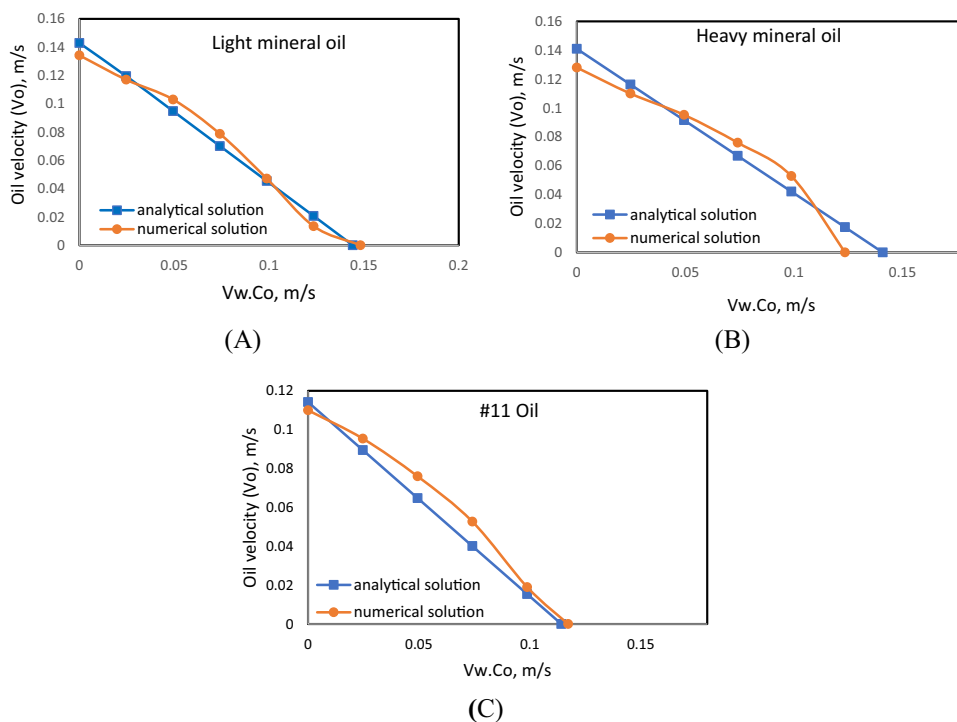
Boundary	Cross-sectional area, mm ²	Setting	Value
Inlet-water	1256	Velocity-inlet	Diverse
Inlet-oil	3.14	Velocity-inlet	Diverse
Outlet	1252.86	Pressure-outlet	2501.55 pa
Wall	–	No slip wall	–

8 s because the time needed for the mixture to completely traverse the separator in all cases is between 2.5 and 5 s (by dividing the separator's length by mix velocity). We think that this period can provide a clear understanding of the separation capacity. All the cases studied in this stage will be done on light mineral oil, and the velocity inside the separator will be less than the critical velocity specified in the first stage ($V_{\text{mix}} < V_{\text{wc}}$).

Case 1 The mixture enters from the inlet, as shown in Fig. 5A, B, according to the inlet velocity of 0.4 m/s (flow rate of 246.3 mm³/s), the oil volume fraction of 0.2, the outlet velocity from the top of 0.04 m/s (flow rate of 50.24 mm³/s), and the outlet from the bottom under a pressure of 2501.55 pa. Meaning that the percentage of exit from the top is 20.39% and the percentage of exit from the bottom (injection) is 79.6%.

The mesh validation check was performed at four values of the number of elements, as shown in Fig. 6; it can be seen that the changes are simple. So, at this stage, we used mesh number 795861 to analyze all cases.

Fig. 4 Comparison of droplet velocities between the numerical and drift-flux models: **A** light mineral oil; **B** heavy mineral oil; **C** #11 oil



Here the separation efficiency for case 1 is 29.05% (the proportion of oil exiting the top outlet to oil entering the separator). Appendix 1 (A–I) shows the water saturation profile for a plane located in the center of the separator during the separation process, and Fig. 7 depicts the water saturation profile to indicate the impacts of inlet velocity during separation. In Fig. 7 (number 1), we can note that the main reason for the decrease in the separation efficiency is the inability of the oil droplets to reach the upper outlet, where the oil droplets collide with the mixture stream, which returns them downward. And it can be observed that the upper outlet is impacted by the inlet velocity Fig. 7(number 2), which scatters the oil droplets and prevents them from exiting, as becomes clearer in the velocity profile in Appendix 1 (J).

Case 2 In this case, we doubled the inlet section area and cut the velocity in half (i.e., the same flow rate); the separation efficiency was 20.16%. Appendix 2 (A–F) illustrates the stages of separation in this case. It is clear that Case 1 had better results than this case. This can be explained by the fact that the mixture's collision with the separator's walls due to its high velocity encourages the separation of oil droplets from the water stream. This behavior is similar to the centrifugation principle, which is the basis for many separators, where high velocity facilitates efficient separation of the oil particles from the water stream.

Case 3 As we said, the main problem with the conventional design in case 1 is that the oil droplets could not get out of the upper outlet. To solve this problem and improve the results of the separator, we proposed a new design, which is a simple modification of the design of Case 1, shown in Fig. 8A–D. The design concept is based on enlarging the size of the mixture

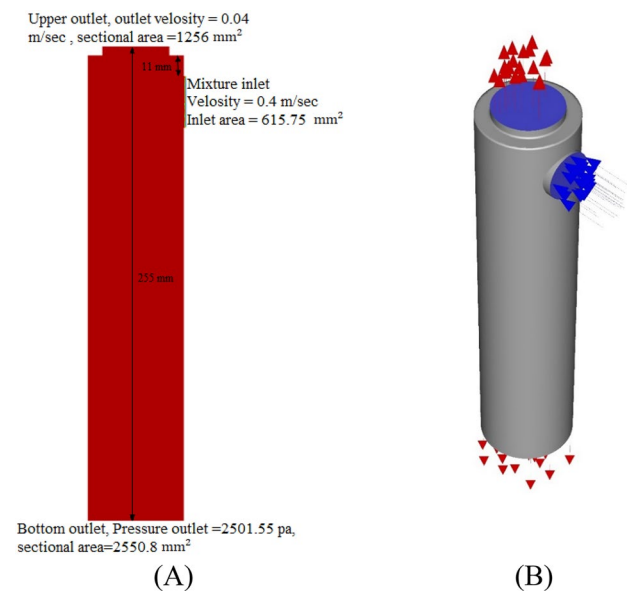


Fig. 5 DOWS geometry of case 1: **A** Dimensions and boundary conditions of DOWS geometry; **B** 3D geometry of DOWS in the simulator

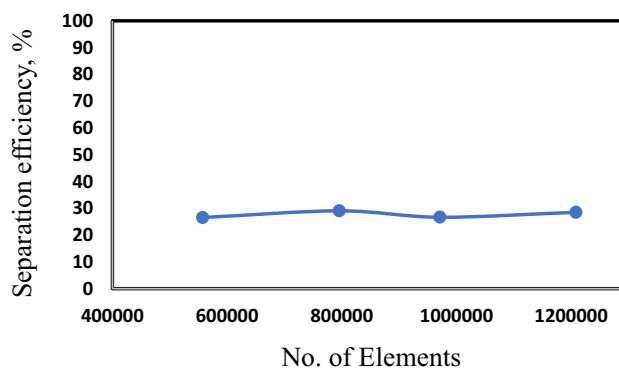


Fig. 6 Mesh independency for case 1

inlet by 15 mm, as shown in Fig. 8B, in order to enable the oil droplets to reach the outlet. In addition, to make the upper outlet area quieter, we lowered the height of the mixture inlet so that the distance between the inlet and the upper outlet is 36 mm and moved the upper outlet as far as possible from the place where the mixture hits the separator walls, as shown in Fig. 8C. Under the same boundary conditions as in Case 1, simulations for Case 3 revealed a separation efficiency of 40.28%, i.e., 38.65% more than for Case 1.

Cases 4, 5, 6, and 7 To understand the effect of the inlet flow rates and the upper outlet flow rates on the separation

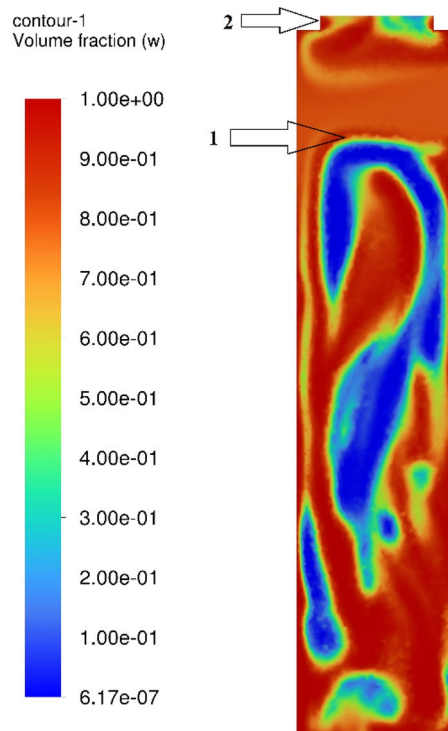


Fig. 7 Contour of the water phase during the separation process; number 1 denotes the region where the stream of the mixture and oil droplets contact; number 2 denotes the impact region of the input mixture on the top outlet area

efficiency, the flow values on the proposed design in Case 3 are studied as follows: Case 4 where the inlet flow is $184.72 \text{ mm}^3/\text{s}$, i.e., the reduction rate is 25%; Case 5 where the inlet flow is $123.15 \text{ mm}^3/\text{s}$, i.e., the reduction rate is 50%; Case 6 where the upper outlet flow rate is $62.8 \text{ mm}^3/\text{s}$, i.e., the increase rate is 25%; and Case 7 where the outlet flow rate is $75.36 \text{ mm}^3/\text{s}$, i.e., the increase rate is 50%. The results of all cases are shown in Table 4.

According to the results of cases 4, 5, 6, and 7, regulating the separator's inlet flow rate improves separator performance more than regulating the upper outlet flow.

Conclusions and future work

This work gives a numerical assessment of the separators used with the DWL approach in order to better understand how well they can separate oil from water and prevent re-injection of oil, which damages the injection region where the effect of flow rates and mixture inlet velocities on separation efficiency

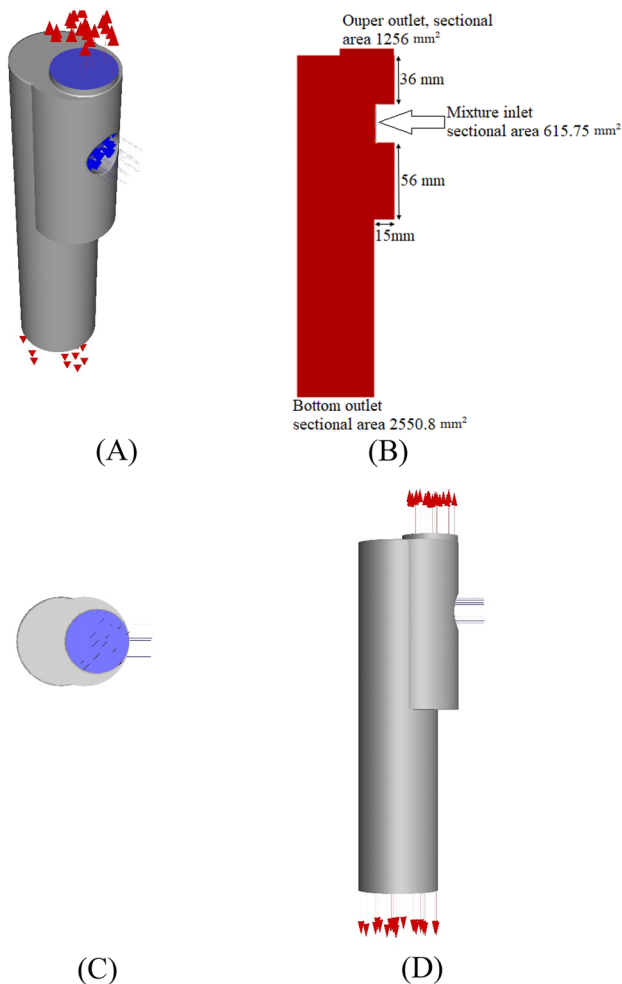


Fig. 8 The proposed design: **A** 3D geometry; **B** geometry dimensions; **C** upper view; **D** side view

was studied, and a novel design that successfully reduces the effect of the mixture inlet velocities was provided. The results of this research can be summarized as follows:

1. At the model validation stage, the outcomes of the commercial numerical simulator used in this work were contrasted with those of the analytical models. The findings demonstrated that when designing two-phase separators, it is viable to rely on commercial simulation to create numerical solutions that are close to the outcomes of the actual separators.
2. In the study of high inlet velocity, the separation efficiency was unsatisfactory, which can be explained by two points. The first is the inability of the oil droplets to exit through the upper outlet, as the oil droplets collide with the mixture stream and are forced to return to the bottom. The second is manifested by the currents generated by the high velocity near the upper outlet, which also prevents oil droplets from leaving.
3. The separation efficiency of low inlet velocity was very poor where the outcomes demonstrate that decreasing the velocity by expanding the inlet section area decreases the separation efficiency. This can be explained by the fact that high-velocity collisions between the mixture and the separator walls aid in the separation of the mixture's oil particles, whereas low-velocity collisions are weak and cause the droplet particles to remain suspended (scattered) in the water stream, making it challenging to form large droplets that can ascend to the upper outlet.
4. The problem of oil droplets not reaching the upper outlet was effectively reduced by the innovative new design, which included an expansion of the mixture entry area and changes to the inlet and outlet positions.
5. According to the findings of the flow rates studied, regulating the separator's inlet flow rate has a more significant impact on separator performance than does regulating the upper outlet flow.
6. In all cases studied in this work, the velocity inside the separator is less than the critical velocity (V_{wc}) calculated analytically, but the complete separation of the oil

Table 4 The separation efficiency results of all cases

	Inlet flow, mm^3/s	Outlet flow, mm^3/s	Separation efficiency (%)
Case 1	246.3	50.24	29.05
Case 2	246.3	50.24	20.16
Case 3	246.3	50.24	40.28
Case 4	184.72	50.24	54.44
Case 5	123.15	50.24	62.76
Case 6	246.3	62.8	43.82
Case 7	246.3	75.36	47.2

droplets did not take place due to the influence of the inlet velocity, which is different in value and direction from the velocity within the separator. So, the analytical models are insufficient to construct this kind of separator because the inlet velocity was not taken into account.

7. The outcomes in all cases are poor. One could argue that gravity separation is ineffective when used alone; thus, in our upcoming work, we'll propose coupling a hydro-

cyclone separator to a gravity separator (separation in two stages) to improve separation efficiency.

Appendix 1

See Fig. 9.

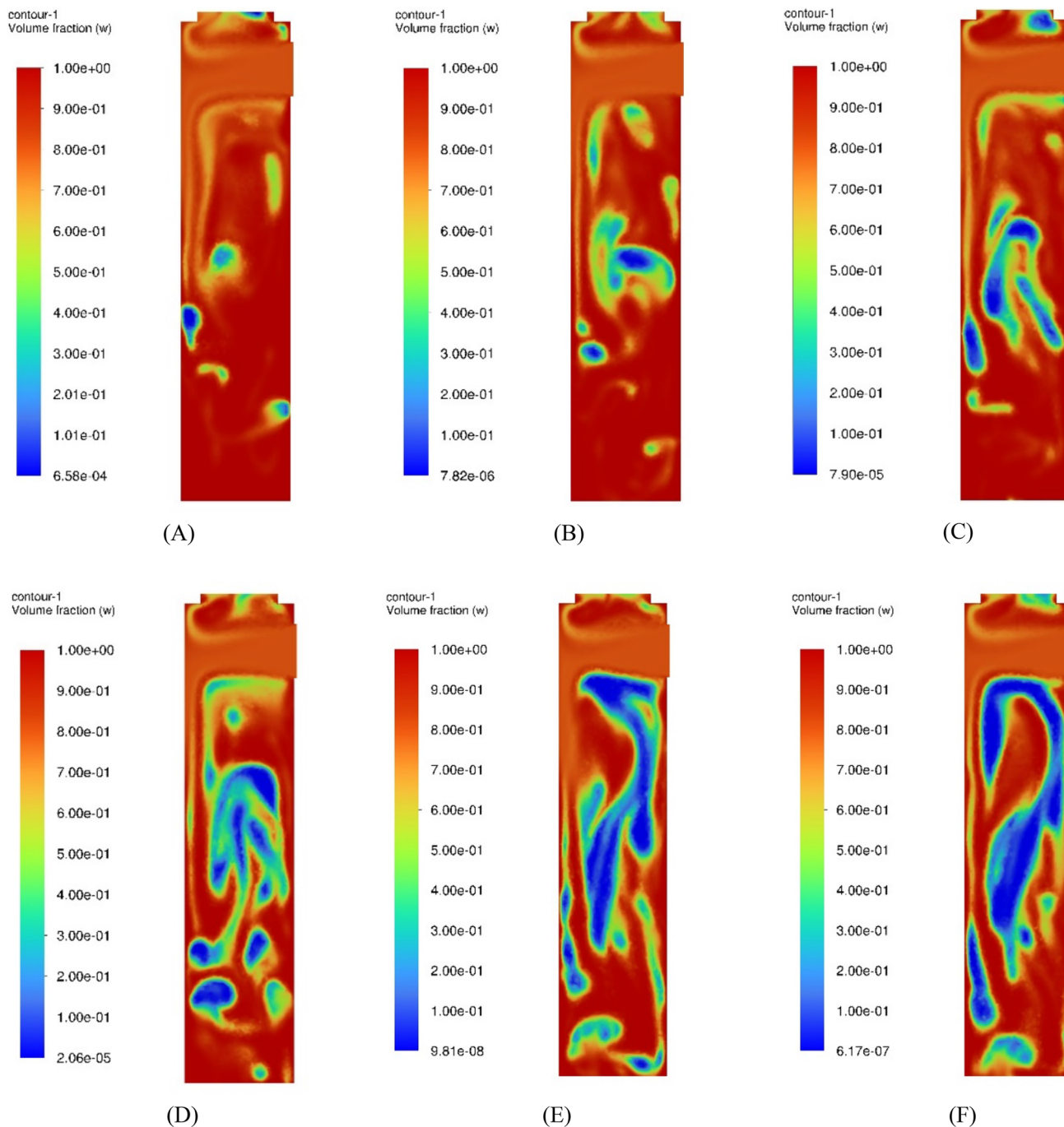


Fig. 9 Demonstrate the phases saturation changes and velocity at case 1 (high-velocity case): **A–I** Contours of the water phase; **J** Contour of velocity

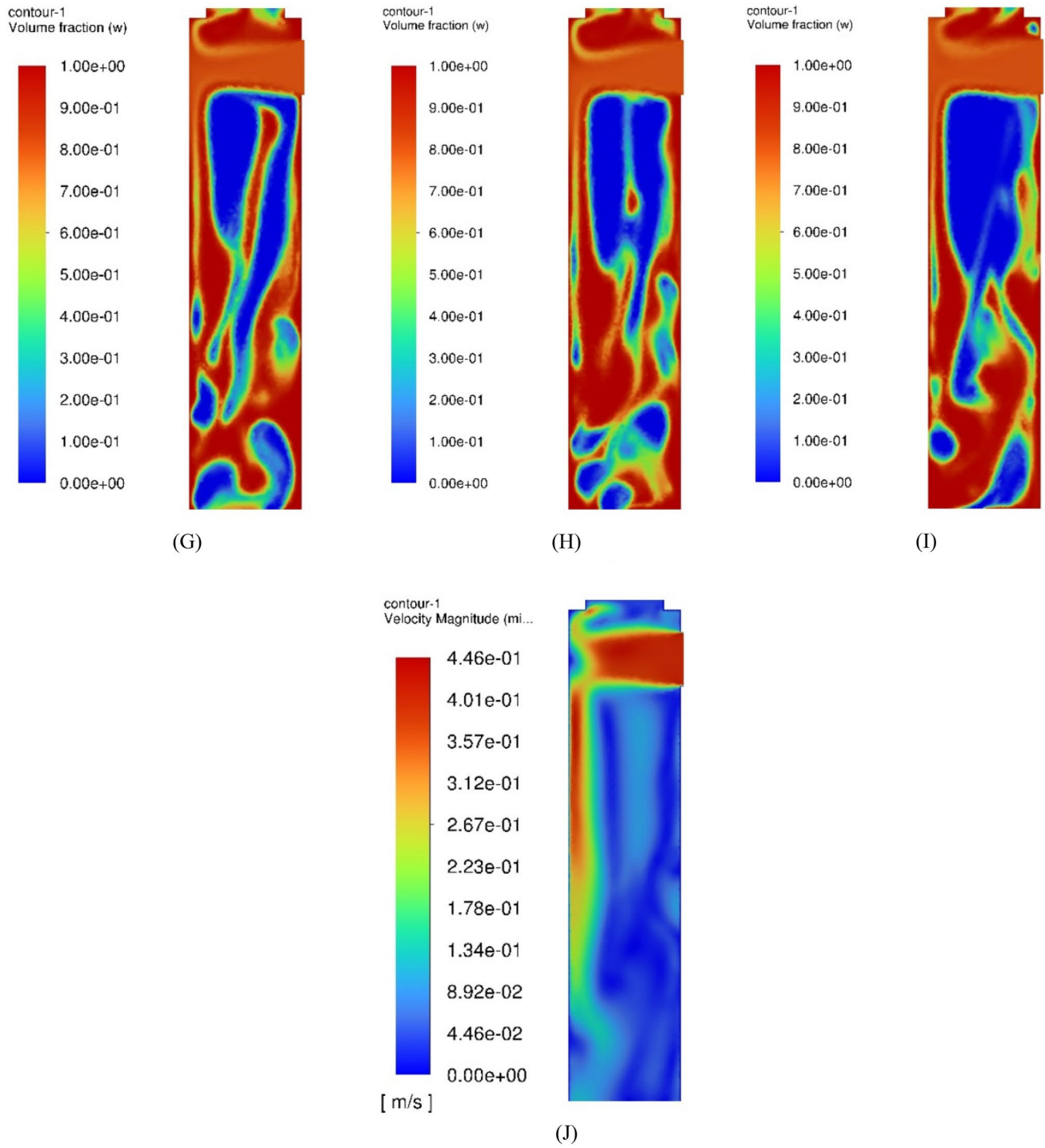


Fig. 9 (continued)

Appendix 2

See Fig. 10.

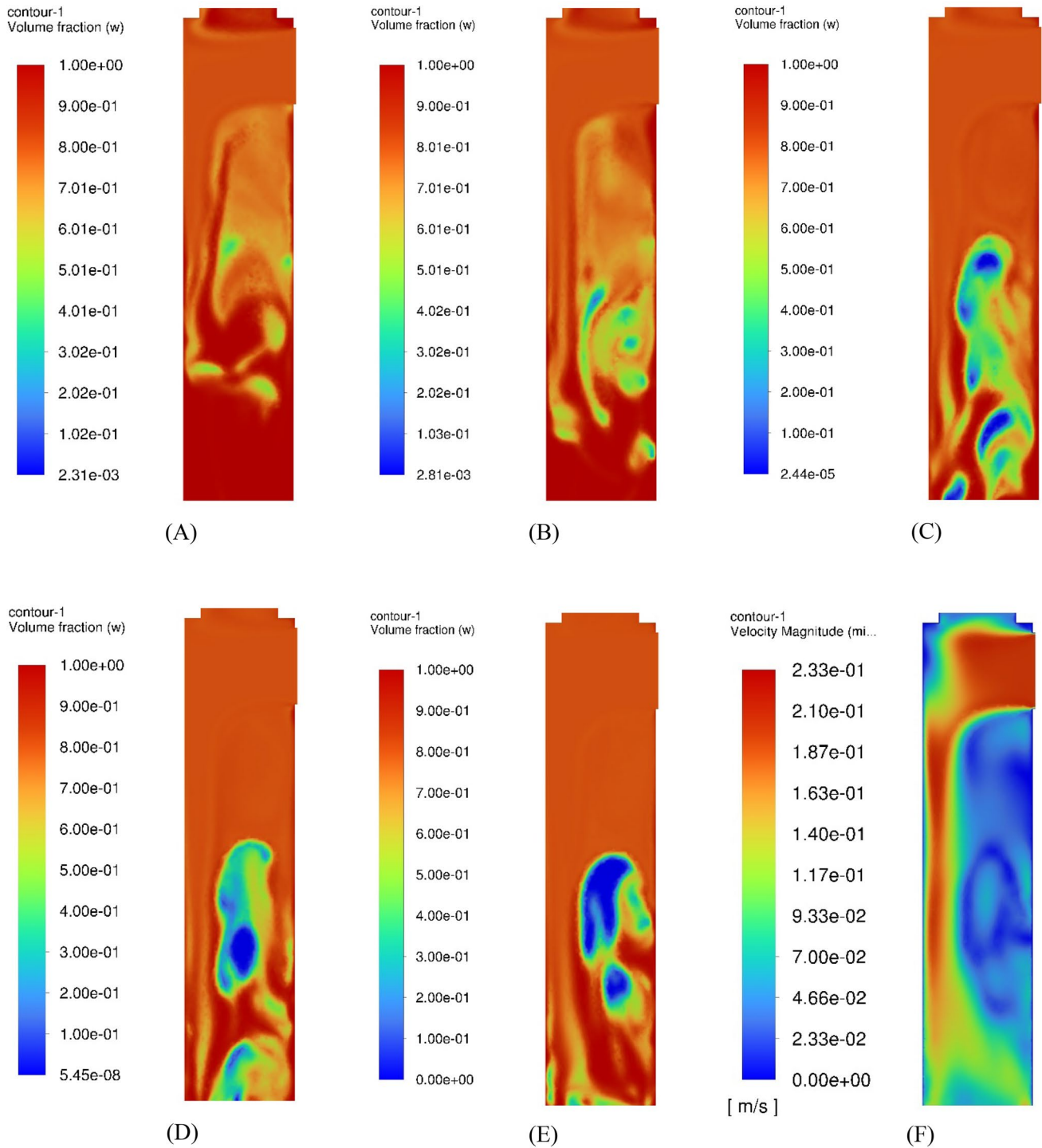


Fig. 10 Demonstrate the phases saturation changes and velocity at case 2 (low-velocity case): **A–E** Contours of the water phase; **F** Contour of velocity

Funding No funding was received for this research.

Data availability Data are confidential and cannot be shared.

Code availability Codes can be shared if requested.

Declarations

Conflict of interest The authors declare that they have no conflict of interest.

Open Access This article is licensed under a Creative Commons Attribution 4.0 International License, which permits use, sharing, adaptation, distribution and reproduction in any medium or format, as long as you give appropriate credit to the original author(s) and the source, provide a link to the Creative Commons licence, and indicate if changes were made. The images or other third party material in this article are included in the article's Creative Commons licence, unless indicated otherwise in a credit line to the material. If material is not included in the article's Creative Commons licence and your intended use is not permitted by statutory regulation or exceeds the permitted use, you will need to obtain permission directly from the copyright holder. To view a copy of this licence, visit <http://creativecommons.org/licenses/by/4.0/>.

References

- Abass H, Bass D (1988) The critical production rate in water-coning system. In: permian basin oil and gas recovery conference <https://doi.org/10.2118/17311-MS>
- Al-Kayiem HH, Osei H, Hashim FM, Hamza JE (2019) Flow structures and their impact on single and dual inlets hydrocyclone performance for oil–water separation. *J Pet Explor Prod Technol* 9:2943–2952. <https://doi.org/10.1007/s13202-019-0690-1>
- Arslan O (2005) Optimal operating strategy for wells with downhole water sink completions to control water production and improve performance. Louisiana State University and Agricultural & Mechanical College, Baton Rouge. https://doi.org/10.31390/gradschool_dissertations.4049
- Arslan O, White C, Wojtanowicz A (2004) Nodal analysis for oil wells with downhole water sink completions. In: Canadian international petroleum conference <https://doi.org/10.2118/2004-242>
- Arslan O, Wojtanowicz A, White C (2003) Inflow performance methods for evaluating downhole water sink completions vs. conventional wells in oil reservoirs with water production problems. In: Canadian international petroleum conference <https://doi.org/10.2118/2003-195>
- Bedrikovetsky P, Da Silva MJ, Fonseca DR, Da Silva MF, Siqueira AG, De Souza A, Furtado C (2005) Well-history-based prediction of injectivity decline during seawater flooding. In: SPE European formation damage conference <https://doi.org/10.2118/93886-MS>
- Bowlin K, Chea C, Wheeler S, Waldo L (1997) Field application of in-situ gravity segregation to remediate prior water coning. In: SPE Western regional meeting <https://doi.org/10.2118/38296-MS>
- Farmen J-E, Wagner G, Oxaal U, Meakin P, Feder J, Jøssang T (1999) Dynamics of water coning. *Phys Rev E* 60:4244
- Ghaffarkhah A, Dijvejin ZA, Shahrabi MA, Moraveji MK, Mostofi M (2019) Coupling of CFD and semiempirical methods for designing three-phase condensate separator: case study and experimental validation. *J Pet Explor Prod Technol* 9:353–382. <https://doi.org/10.1007/s13202-018-0460-5>
- Ghaffarkhah A, Shahrabi MA, Moraveji MK (2018) 3D computational-fluid-dynamics modeling of horizontal three-phase separators: an approach for estimating the optimal dimensions. *SPE Prod Oper* 33:879–895. <https://doi.org/10.2118/189990-PA>
- Guo B, Molinard J, Lee R (1992) A general solution of gas/water coning problem for horizontal wells. In: European petroleum conference <https://doi.org/10.2118/25050-MS>
- Høyland LA, Papatzacos P, Skjæveland SM (1989) Critical rate for water coning: correlation and analytical solution. *SPE Reserv Eng* 4:495–502. <https://doi.org/10.2118/15855-PA>
- Inikori SO, Wojtanowicz AK (2001) Contaminated water production in old oil fields with downhole water separation: effects of capillary pressures and relative permeability hysteresis. In: SPE/EPA/DOE exploration and production environmental conference <https://doi.org/10.2118/66536-MS>
- Jin L (2009) Downhole water loop (DWL) well completion for water coning control---theoretical analysis
- Jin L, Wojtanowicz A (2013) Experimental and theoretical study of counter-current oil–water separation in wells with in-situ water injection. *J Pet Sci Eng* 109:250–259. <https://doi.org/10.1016/j.petrol.2013.08.037>
- Jin L, Wojtanowicz AK (2010a) Coning control and recovery improvement using in-situ water drainage/injection in bottom-water-drive reservoir. In: SPE improved oil recovery symposium <https://doi.org/10.2118/129663-MS>
- Jin L, Wojtanowicz AK (2010b) Performance analysis of wells with downhole water loop installation for water coning control. *J Can Pet Technol* 49:38–45. <https://doi.org/10.2118/138402-PA>
- Jin L, Wojtanowicz AK (2011) Minimum produced water from oil wells with water-coning control and water-loop installations. In: SPE Americas E&P health, safety, security, and environmental conference <https://doi.org/10.2118/143715-MS>
- Jin L, Wojtanowicz AK (2014) Progression of injectivity damage with oily waste water in linear flow. *Pet Sci* 11:550–562. <https://doi.org/10.1007/s12182-013-0371-0>
- Jin L, Wojtanowicz AK, Hughes RG (2010) An analytical model for water coning control installation in reservoir with bottomwater. *J Can Pet Technol* 49:65–70. <https://doi.org/10.2118/137787-PA>
- Johns RT, Lake LW, Ansari RZ, Delliste AM (2005) Prediction of capillary fluid interfaces during gas or water coning in vertical wells. *SPE J* 10:440–448. <https://doi.org/10.2118/77772-PA>
- Nayyar ML (2000) Piping handbook: McGraw-Hill Education
- Ould-amer Y, Chikh S, Naji H (2004) Attenuation of water coning using dual completion technology. *J Pet Sci Eng* 45:109–122. <https://doi.org/10.1016/j.petrol.2004.04.004>
- Refsnes H, Diaz M, Stanko M (2019) Performance evaluation of a multi-branch gas–liquid pipe separator using computational fluid dynamics. *J Pet Explor Prod Technol* 9:3103–3112. <https://doi.org/10.1007/s13202-019-0708-8>
- Safari M, Ameri MJ, Naderifar A (2018) Adaptive control design for a nonlinear parabolic PDE: application to water coning. *Can J Chem Eng* 96:1926–1936. <https://doi.org/10.1002/cjce.23174>
- Shirman EI (1998) Experimental and theoretical study of dynamic water control in oil wells. Louisiana State University and Agricultural & Mechanical College, Baton Rouge
- Swisher M, Wojtanowicz A (1996) In situ-segregated production of oil and water—a production method with environmental merit: field application. *SPE Adv Technol Ser* 4:51–58. <https://doi.org/10.2118/29693-PA>
- Tabatabaei M, Ghalambor A, Guo B (2012) An analytical solution for water coning in vertical wells. *SPE Prod Oper* 27:195–204. <https://doi.org/10.2118/113106-PA>
- Utama FA (2008) An analytical model to predict segregated flow in the downhole water sink completion and anisotropic reservoir. In: SPE annual technical conference and exhibition <https://doi.org/10.2118/120196-STU>
- Widmyer RH (1958) Producing petroleum from underground formations. In: Google Patents.
- Wojtanowicz A, Xu H (1992) A new method to minimize oilwell production water cut using a downhole water loop. In: *CIM* 92–13,

proceedings of the 43rd annual technical meeting of the petroleum society of CIM, Calgary, Canada, June

Wojtanowicz A, Xu H, Bassiouni Z (1991) Oilwell coning control using dual completion with tailpipe water sink. In: SPE production operations symposium <https://doi.org/10.2118/21654-MS>

Zeidani K, White C, Wojtanowicz A (2008) Maximum revenue for oilwells with optimized downhole water drainage. J Can Pet Technol. <https://doi.org/10.2118/08-05-56>

Publisher's Note Springer Nature remains neutral with regard to jurisdictional claims in published maps and institutional affiliations.